Dielectric Spectroscopic Studies on Polypyrrole Glucose Oxidase Films

KUMARAN RAMANATHAN, M. K. RAM, MANJU M. VERGHESE, and B. D. MALHOTRA*

Biomolecular Electronics and Conducting Polymer Research Group, National Physical Laboratory, Dr. K. S. Krishnan Road, New Delhi 110012, India

SYNOPSIS

An investigation was made into the dielectric spectroscopic characteristics of *p*-toluene sulfonate (PTS) doped polypyrrole (PPY) films in the presence and absence of immobilized glucose oxidase (GOX) in three different configurations: Al-PTS-PPY-Al, Al-PTS-PPY/GOX-Al, and Al-PTS-PPY/GOX/β-D-glucose-Al, respectively. Measurement of dielectric loss and capacitance yielded valuable information about the dielectric properties of GOX immobilized in PTS doped PPY films. The effect of both the temperature and varying β-D-glucose concentrations on the mobility of the charge carriers in these films was also systematically studied. © 1996 John Wiley & Sons, Inc.

INTRODUCTION

Recently, there has been increased interest in the development of techniques, such as those based on electrical conductivity and impedance measurements of biological systems, for quantitation and monitoring of specific chemical analytes.[1-7] Enzyme redox reactions operating in biosensors are particularly amenable to interfacing with electrochemical transducers because electron exchange is a key step in the catalytic process.[8-10] In the recent past dielectric measurements contributed to the understanding of the physicochemical processes involved in determining the critical hydration of proteins and enzymes.[1,11-14] The electrical conductivity changes corresponding to enzyme catalysis reaction *in situ* were also highlighted.[15,16] Pethig et al. exploited this concept for the enzyme urease immobilized by crosslinking with glutaraldehyde.[17] The technique has real-time application value in the development of solid-state biosensors used to monitor stored food stuffs, tissues, and seeds.[18,19] The dielectric or impedance measurements are field-dependent phenomena, an important tool for the measurement and evaluation of biomedical/cardiovascular functions.

Several conducting polymers such as polypyrrole (PPY), polycarbazole, and polyaniline are now used for the immobilization of enzymes.[20-25] PPY is well characterized and is probably one of the most suitable polymers for biosensor applications. In the case of third generation biosensors, steady-state amperometric response has been monitored using glucose oxidase (GOX) immobilized onto PPY films. However, the efficiency of the current response obtained from such electrodes due to successful reaction of β-D-glucose with GOX is lower than the expected values. The reduced efficiency of PPY–GOX electrodes can perhaps be attributed to the entrapment of the electronic charges in the various defect levels arising due to the amorphous structure of PPY films.

Motion of a charge carrier in an organic semiconductor under the influence of an electric field results in the formation of an interfacial polarization near the electrodes.[26] The measurements of both the spatial dependence of potential and the space-charge capacitance as a function of applied external potential are likely to reveal valuable information concerning the nature and concentration of charge carriers in a given material. Al with work function of 3.74 eV forms a rectifying contact with PPY having a work function of 4.12 eV.[26-28]

In the present research a systematic investigation was made into space charge polarization studies to monitor the response of a PPY–GOX electrode as

* To whom correspondence should be addressed.

Journal of Applied Polymer Science, Vol. 60, 2309–2316 (1996)
 CCC 0021-8995/96/132309-08

a function of β-D-glucose concentration. The PPY thin films following the entrapment of GOX, and their subsequent treatment with various β-D-glucose concentrations were also studied in the Al–PPY/GOX-β-D-glucose treated Al configuration. The dielectric relaxation studies carried out on Al-PPY/GOX-Al reveal important information about the entrapped charges at various levels in the semiconducting PPY films upon their treatment with various β-D-glucose concentrations.

EXPERIMENTAL

PPY films were grown from aqueous media in a two compartment cell comprising of an indium tin oxide (ITO) coated glass plate as the working electrode and a counterelectrode of platinum (Pt), containing 0.1 *M* pyrrole as monomer and 0.1 *M* sodium salt of *p*-toluene sulfonate (PTS). The self supporting films were grown with the current density of 0.3 mA cm^{-2} for 30–45 min under isothermal conditions in an inert atmosphere. The temperature of the cell was maintained at 4°C. Freestanding films of varying thicknesses from 5–20 μm were carefully detached from ITO glass plates; and the conductivity of the doped PTS–PPY films measured using a 4-point probe method was found to be 1–5 S cm^{-1}. The thickness of the films was kept between 10 and 15 μm and the size of the electrode was 1 cm^2.

The immobilization of GOX on PTS doped PPY was carried out by the physisorption technique. PPY films were in their oxidized state prior to GOX loading. The immobilization was done for varying times extending to about 24 h. Those PPY films containing GOX were subsequently washed with 0.1 *M* phosphate buffer at pH 7.2. It was confirmed that the leaching of GOX adsorbed on the surface of PPY was minimal and the PPY/GOX films could be safely used for further measurements. The activity of GOX physisorbed in the PPY films was estimated by the *o*-dianisidine procedure.[29,30] The current response generated by the oxidation of H_2O_2 at 0.7 V versus the Ag/AgCl reference electrode was monitored after every 100 s using a Keithley electrometer (model 617). The change in response current was monitored as a function of varying β-D-glucose concentration. After the current response measurements, the PPY films were washed several times with deionized water and dried under dynamic vacuum to remove any adsorbed electrolyte from the solution. Al (99.99% pure) contact on either side of PPY films, made by thermal evaporation at a pressure of 10^{-6} torr in the PPY films, was used for the fabrication of the desired configuration.[26]

The capacitance and loss measurements at different frequencies were carried out on Al–PTS–PPY–Al, Al–PTS–PPY/GOX–Al, and Al–PTS–PPY/GOX–β-D-glucose treated Al configurations, respectively, using an HP 4192A impedance analyzer operating within a frequency range from 5 Hz to 13 MHz. The dielectric measurements were performed at a signal voltage of 0.1 V on a 0, 50, 100, and 200 mV dc bias. The measurements were carried out from 1 kHz to 10 MHz.

THEORY

Figure 1(a) depicts the resulting Al–PTS–PPY–Al capacitor. In the presence of a strong bias across the sample, the ions in the sample align toward their respective electrodes. Because the electrodes are blocked, no injection or extraction of charges into

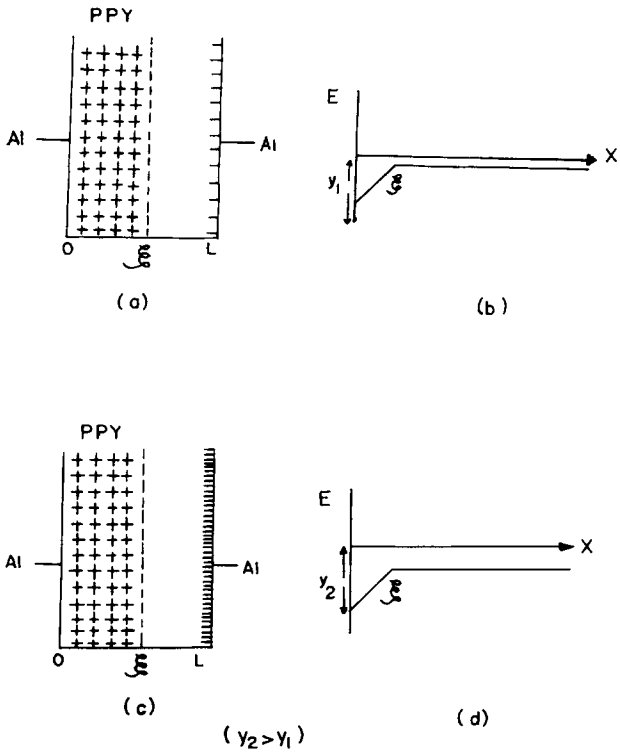

Figure 1 (a) The space charge polarization in PPY films in the Al–PTS–PPY–Al configuration. (b) The charge distribution of the electric field in the Al–PTS–PPY–Al capacitor with the dc bias of 100 mV and ac signal of 0.1 V. (c) Space charge polarization in Al–PTS–PPY/GOX–β-D-glucose treated Al configuration. (d) The field distribution in the Al–PTS–PPY/GOX-β-D-glucose treated Al configuration.

and from PPY films occurs. Thus a space charge is created near the electrodes, resulting in a field gradient across the sample. A depletion region is also created inside the sample. The resulting electric field and charge distribution inside the sample are shown in Figure 1(a–d).

Owing to the blocking nature of our electrodes and an external bias, we were justified in assuming a well defined space–charge region as shown in Figure 1. The equations of motion for the space–charge boundary when an alternating voltage is superposed on the existing bias follow.

As a simplifying assumption, we consider the movement of the space–charge boundary at the cathodic region (this choice is arbitrary). Further, the width of the anodic space–charge region is also ignored as an approximation. The analysis and derivation of polarization based on such an approximation can be found in the literature.[31]

Let the space–charge region be limited to $0 < x < \xi$ as shown in Figure 1. The electric intensity E, in the region $\xi < x < L$, is approximately given by[32]

$$E(\xi) = (1/L)[V_s - (ne/2\epsilon\epsilon_o)\xi^2] \qquad (1)$$

where ϵ_o is the permittivity in free space, e is the magnitude of the electronic charge, ϵ is the high-frequency permittivity, V_s is the static bias across the sample, and n is the concentration of charge carriers.

In a situation where a steady bias is superposed by a small ac component $v = v_o\exp(iwt)$, the capacitance C is given by

$$C = C_\infty[(\alpha^2 + \beta^3)/(\alpha^2 + \beta^2)] \qquad (2)$$

where $C_\infty = \epsilon\epsilon_o A/L$ and A is the area of the electrode. The dielectric loss tangent, tan δ, is given by

$$\tan\delta = \beta(\beta - 1)\alpha/(\beta^3 + \alpha^2) \qquad (3)$$

where α and β are dimensionless variables defined as

$$\alpha = wL^2/2\mu V_s \qquad (4)$$

and

$$\beta = (neL^2/2\epsilon\epsilon_o V_s)^{1/2} = \frac{L}{\xi_s}. \qquad (5)$$

From eq. (3) it is clear that tan δ has a maximum when

$$\alpha^2 = \beta^3 \qquad (6)$$

Finally, from eq. (6), the mobility μ of the charge carriers can be written as

$$\mu = (w_m^4\epsilon^3\epsilon_o^3L^2/n^3e^3V_s)^{1/4} \qquad (7)$$

where w_m is the frequency at which the dielectric loss is maximum and V_s is the static bias across the film.

The treatment of PTS doped PPY–GOX structure with a given β-D-glucose concentration results into the following biochemical reaction:

$$\beta\text{-D-glucose} + \mathrm{GOX_{ox}} \rightarrow \text{gluconolactone} + \mathrm{GOX_{red}} \qquad (8)$$

$$\mathrm{GOX_{red}} + \mathrm{PPY_{ox}} \rightarrow \mathrm{PPY_{red}} + \mathrm{GOX_{ox}} \qquad (9)$$

$$\mathrm{PPY_{red}} \rightarrow \mathrm{PPY_{ox}} + 2e^- \qquad (10)$$

As mentioned earlier, all the free charges (i.e., electrons) resulting from the above biochemical reaction are not found, because some of these fall into the various trap levels of the semiconducting PPY matrix.

Assuming Figure 1(c) is the schematic of the space–charge distribution in an Al–PTS–PPY/GOX–β-D-glucose treated Al capacitor, Figure 1(d) shows the resulting distribution of electric field in an Al–PTS–PPY/GOX–β-D-glucose-Al structure obtained under similar conditions. It can be seen that the formation of a well-defined parallel plate condenser [Fig. 1(c)] occurs following the treatment of PPY–GOX films with β-D-glucose solution. This results in an increase in the electronic charge near the electrode.

RESULTS AND DISCUSSION

Figure 2(a) gives the variation of capacitance as a function of frequency at 100-mV dc bias in the Al–PTS–PPY–Al configuration at room temperature (298 K). The decrease of capacitance with increase in the frequency indicates the presence of interfacial polarization near the electrodes. The resonance behavior observed at nearly 1 MHz for the Al–PTS–PPY–Al structure shows the phenomenon of dipole relaxation in thin PPY films when blocking electrodes are used on either side of the film with an external static bias of 0.1 V. Initially the dielectric loss decreases followed by an increase from 10 kHz to 1 MHz. The presence of dielectric loss peak [Fig. 2(b)] can be attributed to both dipole relaxation and the movement of charge carriers inside the PPY

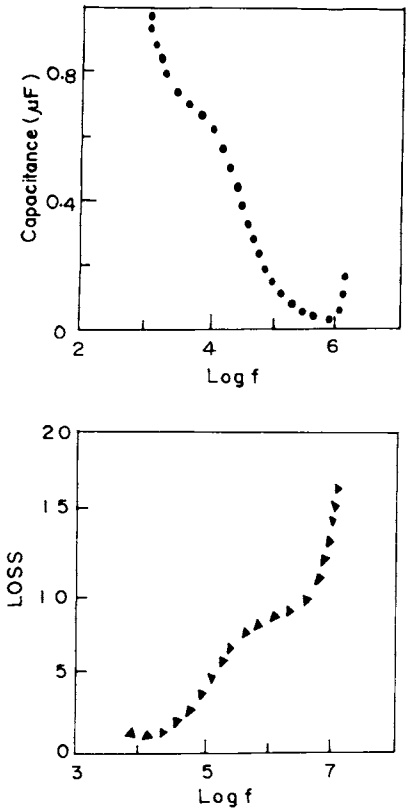

Figure 2 (a) Variation of capacitance as a function of frequency at 100-mV dc bias in the Al–PTS–PPY–Al configuration at 298 K. (b) Variation of loss as a function of frequency at 100-mV dc bias in the Al–PTS–PPY–Al configuration at 298 K.

film. Interestingly, the dipole relaxation is also observed nearly at the same frequency (1 MHz) at which the capacitance curve [Fig. 2(a)] shows the resonance behavior. Because the various configurations were measured at the intermediate frequency region, the Maxwell–Wagner polarization effect does not come into effect.

Figure 3(a) exhibits the variation of capacitance as a function of frequency for the Al–PTS–PPY–GOX–Al configuration and Al–PTS–PPY–GOX–β-D-glucose treated Al configurations. It can be seen in Figure 3(a) (curve 1) that the immobilization of GOX in PPY films results in the increased value of the capacitance. Figure 3(a) (curve 2) shows the variation of the capacitance as a function of frequency in the Al–PTS–PPY/GOX–β-D-glucose treated (10 mM) Al structure. The value of the capacitance shows an increase due to the availability of a larger number of free charges in the PPY matrix following the treatment of the PTS–PPY/GOX structure with β-D-glucose solution (10 mM). Figure 3(b) (curve 1) depicts the shift of the loss peak observed at 1 MHz. This shift of the dielectric loss peak includes the capacitance resonance that can be due perhaps to the increased number of induced dipoles in the Al–PTS–PPY/GOX–Al configuration. The emergence of an additional loss peak at 100 kHz can be attributed to the existence of the intrinsic dipoles of GOX present in the PPY matrix. The electronic charges liberated due to the treatment of PTS–PPY/GOX structure with a given β-D-glucose solution are not likely to be sensed because of the trapping of some of the charges at the various defect levels of the PPY matrix. These electronic charges are well separated from the conjugational defects under the influence of both static bias and the applied ac signal, resulting in the formation of a well-defined parallel plate condenser as shown in Figure 1(c). The shift from 1 to 2 MHz in Figure 3(b) (curve 2), the dielectric loss peak, can be ascribed to the presence of an increased number of induced dipoles after its treatment with β-D-glucose

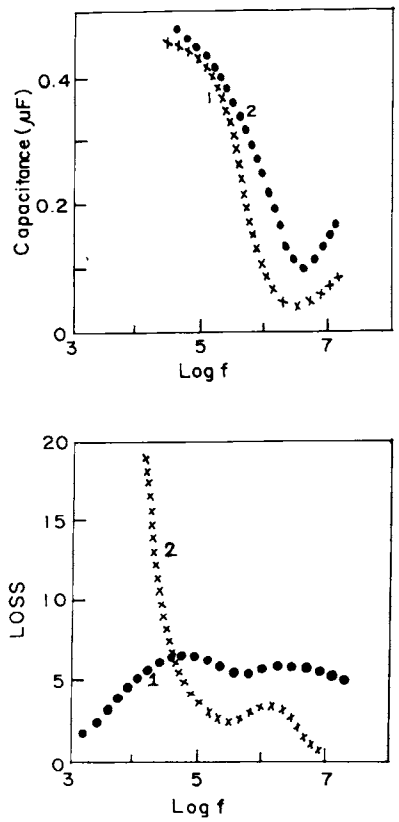

Figure 3 (a) Variation of capacitance as a function of frequency at 100-mV dc bias in the Al–PTS–PPY/GOX–Al structure (curve 1) and the Al–PTS–PPY–GOX–β-D-glucose treated (10 mM) Al structure (curve 2). (b) Variation of dielectric loss as a function of frequency at a 100-mV dc bias in the Al–PTS–PPY–GOX–β-D-glucose treated (10 mM) Al structure (curve 2).

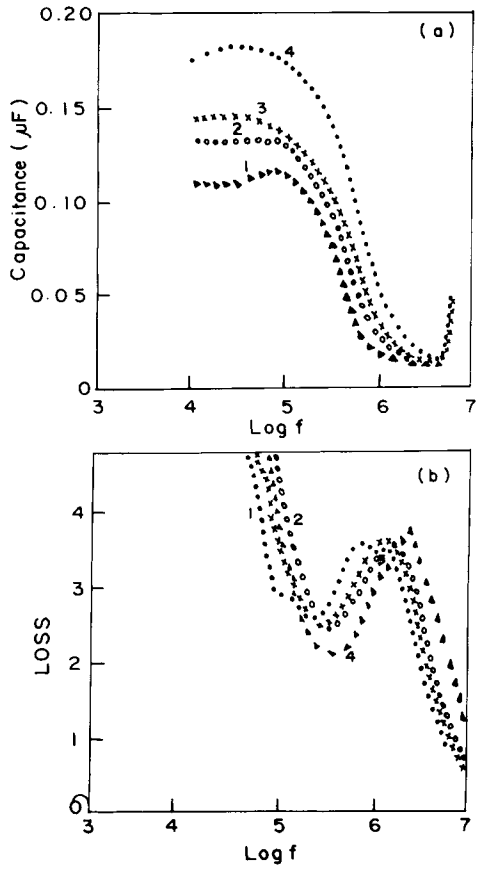

Figure 4 (a) Variation of capacitance with frequency as a function of dc bias in Al–PTS–PPY/GOX–β-D-glucose treated (10 m*M*) Al: curve 1, 0 mV; curve 2, 50 mV; curve 3, 100 mV; curve 4, 200 mV dc biases, respectively. (b) Variation of loss with frequency as a function of dc bias in the Al–PTS–PPY/GOX–β-D-glucose treated (10 m*M*) Al configuration: curve 1, 0 mV; curve 2, 50 mV; curve 3, 100 mV; and curve 4, 200 mV dc biases, respectively.

concentration (10 m*M*) in the above configuration. The observed gradual decrease of the dielectric loss at 100 kHz arises due to the presence of a large number of free charges that are responsible for the decrease in the number of intrinsic dipoles of the GOX in the above configuration.

The variation of capacitance as a function of frequency observed for the Al–PPY/GOX–β-D-glucose treated (10 m*M*) Al configuration at bias voltages of 0, 50, 100, and 200 mV dc bias was systematically measured and are shown in Figure 4(a) (curves 1–4). The observed increase in the value of capacitance [Fig. 4(a)] with the increase in bias voltage from 0 to 200 mV is due to the increase in the density of charge carriers in the space-charge region in the above configuration. The shift (1.2 MHz) of the loss peak as seen in Figure 4(b) (curves 1–4) indicates the increased number of the induced dipoles arising as a result of polarization of PPY molecules containing the immobilized GOX.

Figure 5(a) shows the variation of capacitance as a function of frequency for varying concentrations of β-D-glucose, viz., 10, 20, 40, and 80 m*M*, on PPY containing physisorbed GOX. There is a marked increase in the value of capacitance brought about as a result of the reaction with β-D-glucose of the GOX immobilized in PPY films. Figure 5(b) is the variation of dielectric loss obtained as a function of frequency for varying concentrations of β-D-glucose, viz., 10, 20, 40, and 80 m*M*, on PPY/GOX films. It is interesting to see [Fig. 5(b)] that the intensity of the observed dielectric loss peak increases in the Al–PTS–PPY/GOX–β-D-glucose treated Al structure. The increase in the magnitude of the dielectric

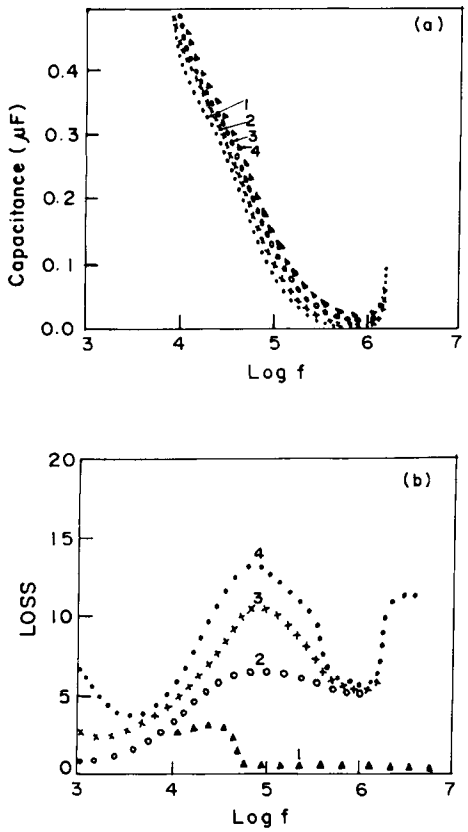

Figure 5 (a) Variation of capacitance (μF) with frequency as a function of β-D-glucose concentration in the Al–PTS–PPY/GOX–β-D-glucose treated Al configuration: curve 1, 10 m*M*; curve 2, 20 m*M*; curve 3, 40 m*M*; curve 4, 80 m*M*, respectively. (b) Variation of loss with frequency as a function of β-D-glucose concentration in the Al–PTS–PPY/GOX–glucose treated Al configuration: curve 1, 10 m*M*; curve 2, 20 m*M*; curve 3, 40 m*M*; and curve 4, 80 m*M*, respectively.

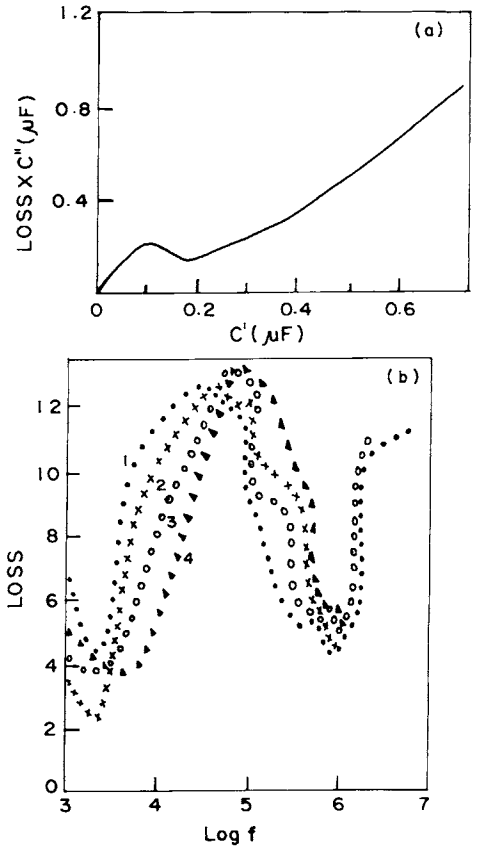

Figure 6 (a) Cole–Cole plot for the Al–PTS–PPY/GOX–β-D-glucose treated (80 m*M*) Al configuration. (b) Variation of loss with frequency as a function of temperature: curve 1, 30°C; curve 2, 40°C; curve 3, 50°C; and curve 4, 60°C, respectively.

loss peak at 100 kHz can be understood to arise from the increased number of induced dipoles formed due to polarization of GOX molecules. Figure 6(a) is the Cole–Cole plot obtained as a result of capacitance measurements on the Al–PTS–PPY/GOX–β-D-glucose (10 m*M*) treated Al configuration. The marked deviation from semicircular arc to scew type as shown in Figure 5(a) points out the presence of complex relaxation behavior in this system arising from the presence of charge carriers and their conductivity behavior. We can express the complex permittivity ϵ^* by the following equation:

$$\epsilon^* = \epsilon_\infty + [(\epsilon_o - \epsilon_\infty)/1 + iw\tau] - i\sigma w \quad (11)$$

where ϵ_o is the static dielectric constant, τ is the relaxation time, ϵ_∞ is the instantaneous dielectric permittivity, σ is the conductivity of the medium, and w is the angular frequency. The observed scew-type behavior came from the conduction of various charge carriers. The presence of two relaxation times τ_1 and τ_2 can be clearly seen in the Cole–Cole plot. The values of relaxation times τ_1 and τ_2 were calculated to be 2.6 and 0.14 μs, respectively. Figure 6(b) exhibits the variation of dielectric loss as a function of frequency at different temperatures, viz., 30, 40, 50, and 60°C. The relaxation phenomena observed in the loss curve is possibly due to the damping of the dipole oscillators at 2 MHz. Although the shapes of the loss profiles are similar, the shift in the frequency at which the dielectric loss maximum occurs can perhaps be attributed to the change in the value of mobility of the charge carriers. Such a decrease in the value of the loss peak in the PPY system may be due to the negative temperature coefficient of the charge carriers present in the PPY.

To further understand the behavior of the trapped charges, the amperometric response of the PPY–GOX electrode was ascertained with varying concentrations at different temperatures. Figure 7 is the variation of the current response with varying β-D-glucose concentrations recorded in the temperature range 10–60°C at a pH of 6.5. The response current increases with increasing glucose concentrations at a given temperature and also increases with increasing temperature for a given β-D-glucose concentration. The apparent decrease in the value of the current beyond this temperature, $T > 50$°C, with varying glucose concentrations can perhaps be attributed to the conformational changes in GOX molecules occurring in PPY matrix.

Based on eq. (7) an attempt was made to compute the magnitude of the mobility of the charge carriers. Figure 8(a) shows the variation of mobility as a function of temperature. There is a linear decrease in the value of mobility of the charge carriers with an increase in temperature in the PTS–PPY/GOX–

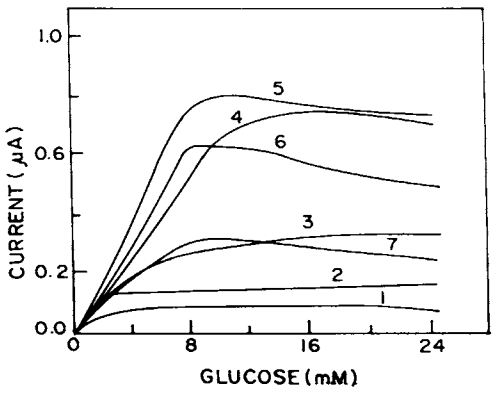

Figure 7 Variation of current response with varying β-D-glucose concentration as a function of temperature: curve 1, 10°C; curve 2, 20°C; curve 3, 30°C; curve 4, 40°C; curve 5, 50°C; curve 6, 54°C; curve 7, 60°C, respectively.

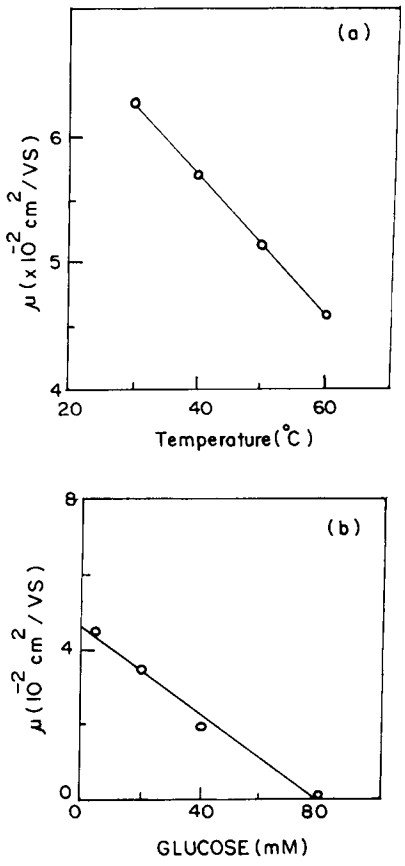

Figure 8 (a) Variation of mobility (μ) as a function of temperature. (b) Variation of μ as a function of β-D-glucose concentration in Al–PTS–PPY–GOX/β-D-glucose treated Al configurations.

β-D-glucose treated Al structure. Figure 8(b) shows the variation of mobility obtained as a function of β-D-glucose concentration. The observed decrease in the value of the mobility μ with β-D-glucose concentration indicates the increased number of charge carriers, arising due to the enzymatic (GOX) reaction in semiconducting PPY. The observed decrease in the mobility of the charge carriers with an increase in the β-D-glucose concentration in the Al–PPY/GOX–β-D-glucose treated Al configuration can perhaps be due to the existence of electrostatic repulsion due to the increased number of free charges.

CONCLUSIONS

The results of the systematic dielectric measurements carried out on various configurations of Al–PTS–PPY/GOX–Al systems clearly demonstrate the existence of loss peaks at 100 kHz and 2 MHz due to the formation of intrinsic dipoles arising from the polarization of GOX and PTS–PPY molecules, respectively. Further, the mobility of the charge carriers was estimated to be 10^{-2} cm^2 V^{-1} s^{-1} in the Al–PPY/GOX–β-D-glucose treated Al structure. On the basis of the model based on interfacial polarization, various studies showed that the electrons emanating from the biochemical reaction of β-D-glucose with GOX physisorbed on PTS–PPY films get trapped in the semiconducting PPY and consequently influences the observed amperometric response of the enzyme electrode.

In light of the above measurements, it should be interesting to carry out systematic studies with regard to applications of PTS doped PPY films for sensing of various biochemical parameters such as urea, cholesterol, and creatinine using dielectric relaxation measurements.

We are grateful to Prof. E.S.R. Gopal, Director, NPL, for his continued interest and constant encouragement in this work. We also wish to thank Dr. Subhas Chandra for his interest in this work. Two of us (K.R. and M.K.R.) thank the CSIR for financial support. Thanks are due to Dr. N. S. Sundaresan and Dr. R. Mehrotra for their valuable suggestions in the preparation of this manuscript. Financial support from the Department of Science and Technology (Project TSD/DST/F121) is gratefully acknowledged.

REFERENCES

1. R. Pethig, *Ann. Rev. Phys. Chem.*, **43,** 177 (1992).
2. D. W. Pierce and S. G. Boxer, *J. Phys. Chem.*, **96,** 5560 (1992).
3. H. Morgan and R. Pethig, *J. Chem. Soc., Faraday Trans. I,* **82,** 143 (1986).
4. L. L. Hause, R. A. Komorowski, and F. Gayon, *IEEE Trans. Biomed. Eng.*, **28,** 403 (1981).
5. T. W. Athey, M. A. Stuchly, and S. S. Stuchly, *IEEE Trans. Microwave Theor. Tech.*, **30,** 82 (1982).
6. E. C. Burdette, F. C. Cain, and J. Seals, *IEEE Trans. Microwave Theor. Tech.*, **28,** 414 (1980).
7. A. K. Jonscher, *Nature,* **253,** 717 (1975).
8. E. Tamiya, I. Karube, S. Hattori, M. Suzuki, and L. K. Yokohama, *Sensors Actuators,* **18,** 297 (1987).
9. J. S. Schultz, *Vigyan Sci. Am.*, **September,** 54 (1991).
10. N. C. Foulds and C. R. Lowe, *J. Chem. Soc. Faraday Trans. I,* **82,** 1259 (1986).
11. K. L. Nagai, A. K. Jonscher, and C. T. White, *Nature,* **277,** 185 (1979).
12. X. Bowang, Y. Huang, R. Holzel, J. P. H. Hart, and R. Pethig, *J. Phys. D, Appl. Phys.*, **26,** 312 (1993).
13. B. A. Lawton and R. Pethig, *Meas. Sci. Technol.*, **4,** 38 (1993).

14. B. A. Lawton and R. Pethig, *Meas. Sci. Technol.*, **4,** 226 (1993).
15. W. J. Albery, P. N. Bartlett, and D. H. Craston, *J. Electroanal. Chem.*, **194,** 224 (1985).
16. A. E. G. Cass, G. Davis, and G. D. Francis, *Anal. Chem.*, **56,** 667 (1984).
17. J. A. R. Price, J. P. H. Burt and R. Pethig, *Biochim. Biophys. Acta,* **964,** 221 (1988).
18. L. B. Wingard, J. G. Scheller, and S. K. Wilson, *J. Biomed. Mater. Res.*, **13,** 921 (1979).
19. D. L. Wise, Ed., *Applied Biosensors,* Butterworth Publishers, Stoneham, MA, 1989, p. 227.
20. N. C. Foulds and C. R. Lowe, *J. Chem. Soc. Faraday Trans. I,* **82,** 2159 (1986).
21. K. Ramanathan, S. Annapoorni, A. Kumar, and B. D. Malhotra, *J. Mater. Sci. Lett.*, **15,** 124 (1996).
22. M. M. Verghese, N. S. Sundaresan, T. Basu, and B. D. Malhotra, *J. Mater. Sci. Lett.*, **14,** 401 (1995).
23. H. Shinohara, H. T. Chiba, and M. Aizawa, *Sensors Actuators,* **13,** 79 (1988).
24. J. C. Cooper and E. A. H. Hall, *Biosens. Bioelectron.*, **7,** 473 (1992).
25. K. Ramanathan, S. Annapoorni, and B. D. Malhotra, *Sensors Actuators B* (Chem.), **21,** 165 (1994).
26. N. N. Beladakere, S. C. K. Misra, M. K. Ram, D. K. Rout, R. Gupta, B. D. Malhotra, and S. Chandra, *J. Phys. Condensed Matter,* **4,** 5747 (1992).
27. S. C. K. Misra, M. K. Ram, S. S. Pandey, B. D. Malhotra, and S. Chandra, *Appl. Phys. Lett.*, **60,** 1219 (1992).
28. S. S. Pandey, S. C. K. Misra, B. D. Malhotra, and S. Chandra, *J. Appl. Polym. Sci.*, **44,** 911 (1992).
29. J. Hu and A. P. F. Turner, *Anal. Lett.*, **24,** 15 (1991).
30. A. P. F. Turner, I. Karube, and G. S. Wilson, Eds., *Biosensors: Fundamentals and Applications,* Oxford Univ. Press, Oxford, UK, 1987.
31. R. Coelho, *Physics of Dielectrics for the Engineer,* Elsevier, Amsterdam, 1979.
32. A. von Hippel, E. P. Gross, J. G. Gelatis, and M. Geller, *Phys. Rev.*, **91,** 568 (1953).

Received August 22, 1995
Accepted November 5, 1995